InterPore JOURNAL

Original Research

EXPERIMENTAL STUDY OF MICROBIAL HYDROGEN CONSUMPTION RATES BY *OLEIDESULFOVIBRIO ALASKENSIS* IN POROUS MEDIA

Raymond Mushabe[1], Na Liu[1], Nicole Dopffel[2], Geir Ersland[1], Martin A. Fernø[1,2]

[1]*Department of Physics, and Technology, University of Bergen, Bergen, Norway;* [2]*Norwegian Research Center AS – NORCE, Bergen, Norway*

Correspondence to:
Raymond Mushabe,
ramus8091@uib.no

How to Cite:
Mushabe, R., Liu, N., Dopffel, N., Ersland, G., & Fernø, M. A. Experimental Study of Microbial Hydrogen Consumption Rates by Oleidesulfovibrio Alaskensis in Porous Media. *InterPore Journal*, *2*(2), IPJ040625–3. https://doi.org/10.69631/ipj.v2i2nr72

RECEIVED: 12 Dec. 2024
ACCEPTED: 27 Apr. 2025
PUBLISHED: 4 Jun. 2025

ABSTRACT

The recovery efficiency of short- and long-term cyclic operations of porous media underground hydrogen storage (UHS) is a key parameter for successful implementation, but anaerobic microbes autochthonous in the storage formation can consume hydrogen and adversely influence hydrogen recoverability and storage efficiency. Here we have experimentally measured hydrogen consumption rates by a model sulphate-reducing bacterium (*Oleidesulfovibrio alaskensis* G20) in drainage-storage cycles that mimic porous media UHS. Laboratory tests were performed in cylindrical sand pack columns as storage site analogues (inner diameter: 14.7 mm, length: 51.4 mm) with an average porosity of 28% at conditions of 37°C and 1.15 bara. The storage capacity (initial hydrogen saturation in place) of each sand pack was also analyzed and compared against sterilized benchmarks. We observed an exponential decay in microbial hydrogen consumption between storage cycles: 28 ± 12% hydrogen was lost during the first cycle (with a peak average rate of 1.26 ± 0.12µmol/hr/cm^3), compared with 10 ± 5% in the second cycle and 7 ± 3% in the third cycle. The cumulative loss across the three cycles amounted to 15 ± 6%, even though nutrient and carbon source concentrations were adequate for full hydrogen consumption in each cycle. The reduced microbial activity after the first storage cycle was explained by the observed increase in brine pH from an initial 7.5 to 8.4 ± 0.2 at the end of the last storage cycle. We observed improvement in the average hydrogen in place saturations after the first non-sterile storage cycles. Our experimental data enhances the understanding of microbial hydrogen loss during UHS and its impact on recovery and storage efficiency.

KEYWORDS

Underground hydrogen storage, Microbial hydrogen consumption, Anaerobic sulphate reduction, pH, Storage capacity, Cyclic drainage and storage

@2025 The Authors

This is an open access article published by InterPore under the terms of the Creative Commons Attribution-NonCommercial-NoDerivatives 4.0 International License (CC BY-NC-ND 4.0) (https://creativecommons.org/licenses/by-nc-nd/4.0/).

1. INTRODUCTION

The need to address the energy/climate dilemma has triggered an increase in the share of renewable energy in the last two decades, especially electricity from solar and wind (45). This trend is anticipated to continue in the next decades (45, 43). However, these renewable energy supplies are inherently intermittent. Underground hydrogen storage (UHS) is currently seen as a technology that can tackle the imbalance between supply and demand from renewable energy sources (31). Excess electrical energy can be converted into hydrogen, stored in subsurface porous reservoirs, and later recovered to generate electricity when needed. (2, 15, 20, 31, 37, 38). However, many subsurface microorganisms in potential storage sites such as aquifers or depleted hydrocarbon reservoirs can consume the stored hydrogen and alter the gas composition (12, 40, 41). In the context of UHS, it is important to understand the microbial processes that will be triggered or accelerated during introduction of high concentrations of hydrogen in the porous medium (11). However, microbes can only access and consume aqueous hydrogen above a threshold aqueous concentration (12, 13, 26, 40). The process is hence dependent on the solubility of hydrogen in water (0.00014 g/kgw) (5, 6, 18), which stays relatively low at a wide range of pressure conditions. For hydrogenotrophic sulphate reduction, hydrogen solubility at storage conditions exceeds the threshold concentration value (1-15 nM H_2) (40) that triggers the reaction. It has been known for over 100 years that heterotrophic sulfate reduction occurs (10, 28), but the specific kinetics and effects related to subsurface hydrogen storage in porous media are still underexplored. Recently, several controlled batch and flow experiments have been conducted to quantify the kinetics of hydrogenotrophic sulphate reduction and explicitly characterize the resulting gas composition (11, 13, 21, 40). Specifically, one study (13) looked at one sulphate reducer (*Desulfohalobium retbaense*) and one halophilic methanogen (*Methanocalculus halotolerans*) at pressures a few mbar above atmospheric pressure and 37°C. It was observed (13) that hydrogen was consumed by both microbial strains, with the consumption rate by the sulphate reducer strain being partially dependent on the hydrogen concentration. The work by Thaysen et al (40) on formation brines containing anaerobic sulphate reducers at the same temperature conditions and 2.5 bara showed similar results. The calculated and reported bulk hydrogen consumption rates were 0.62 ml/day (or 0.04 µmol/hr/ml) by Dopffel et al (13), and 0.09 µmol/hr/ml by Thaysen et al (40). Liu et al (21) studied *D. retbaense* at an elevated pressure (35 barg), and reported that 29.4% of the initially stored hydrogen was consumed within two days of incubation at a peak consumption rate of 0.042 µmol/hr or (8.2 µmol/(hr.ml). During these studies, pH significantly influenced bacterial growth and hydrogen consumption rates. Hydrogen was rapidly consumed at a pH near 7, however consumption ceased as the pH increased to approximately 9. A recent bulk study by Dohrmann et al (11) also showed that microbial hydrogen consumption was primarily dependent on the brine pH and hydrogen concentration, with a peak consumption rate of 0.014 µmol/(hr.ml) at ambient pressure and 30°C. The increase in pH (11, 13) was attributed to proton loss due to hydrogenotrophic sulphate reduction (26, 40) as illustrated in **Equation 1**, despite the reaction products (H_2S and HS^-) releasing protons from partial dissociation in brine, as shown in **Equation 2** and **Equation 3**.

$$4H_2 + SO_4^{2-} + 2H^+ \rightarrow H_2S + 4H_2O \quad -38\,kJ/mol(H_2) \tag{1}$$

$$H_2S \leftrightharpoons HS^- + H^+ \tag{2}$$

$$HS^- \leftrightharpoons S^- + H^+ \tag{3}$$

However, to accurately quantify microbial hydrogen consumption in porous media, core scale data sets are necessary for both potential reservoir characterization and provision of quality input data to numerical models. Most of the recent core scale studies on UHS have focused on fluid-fluid and fluid-rock interactions during hydrogen injection (drainage) and withdrawal (imbibition) without microbial cells in the aqueous phase.

To fill the existing knowledge gap in core scale studies, our study focusses on understanding and quantifying anaerobic microbial hydrogen consumption in sand pack columns. Our study mimics

storage scenarios with hydrogen as the only gas, saturating sandstone reservoirs pores together with bacteria-containing brine. The effect of hydrogen replenishment through drainage cycles on microbial hydrogen consumption is further studied. Additional objectives were to study the effect of bacteria growth and hydrogen consumption on the porous media storage capacity and injectivity. The bacterial strain used was *Oleidesulfovibrio alaskensis* G20 (DSM 17464), which thrives best at 37°C–40°C and a wide range of pressure in an anoxic environment. This bacteria strain was first discovered in an oil field in Alaska (14). The study findings provide additional knowledge that can be used for further screening of potential porous media storage sites for hydrogen.

2. METHODS AND MATERIALS

2.1. Porous medium

Sand pack columns prepared with sand purchased from a commercial supplier (AGSCO) were used in the study. The sand was manually sieved from the supplied sand stock to an average grain size of 425 µm and treated with a strong acid (0.6 M hydrochloric acid) to remove impurities (predominately calcite). The acid was neutralized with NaOH, and the sand was rinsed with deionized water (DI) in a sonic bath to a pH range between 7–7.5, before drying at 60°C and autoclaved at 121°C for 20 minutes. The sand was packed in a cylindrical polyetheretherketone (peek) sand pack holder (inner chamber 15 mm x 60 mm) (See **Fig. S1** in the **Supplementary Material**, available online). The sand packs were prepared wet in DI, with sand grains added in successive layers. A compressive force of 30 N was applied between each step to compact the sand. All sand packs had an average porosity of 28%, a uniform specific surface area (SSA) of 76 cm^2/cm^3, and an average sand grain density of 2.55 g/cm^3. The SSA was estimated using the correlation developed by Rabbani et al (29) as shown in **Equation 4**. The specific area was considered to provide a measure of fluid-grain contact in the sand packs. The sand pack absolute permeability was measured by injecting 2 pore volumes (PVs) of degassed deionized water at 30 cm^3/hr and 45 cm^3/hr with the sand pack in a horizontal position. **Table 1** summarizes sand pack permeabilities and identities.

$$\boldsymbol{SSA = 4.23\frac{(1-\Phi)}{d}} \tag{4}$$

Above, $\boldsymbol{\Phi}$ is the sand pack porosity, $\boldsymbol{d}$ is the average grain size in cm (defined by the diameter of the mesh used to sieve the sand), and $\boldsymbol{SSA}$ is the calculated specific surface area in cm^2/cm^3. The formulation assumes that the sand grains are spherical.

Table 1: Summary of key sand pack properties and the experimental routine. All sand packs were uniformly prepared, with a pore volume of 2.44 cm^3, average sand grain diameter of 425 µm, and a specific surface area of 76 cm^2/cm^3. The variation in permeability was attributed to grain packing. All sand packs were initially pressurized to 1.15 bara at the start of each storage cycle except for BSP8 which was pressurized to 1.6 bara and BSP7 to 1.75 bara in the fifth cycle.

ID	Test type	Absolute permeability [Darcy]	*Number of Cycles for:*		Initial shut-in pressure [bara]
			Drainage	Storage	
SSP1	Sterilized	3.4	3	3	1.15
SSP2	Sterilized	8.2	3	3	1.15
SSP3	Sterilized	6.6	3	3	1.15
BSP1	Bacterial	3.5	3	3	1.15
BSP2	Bacterial	9.0	3	3	1.15
BSP3	Bacterial	7.1	3	3	1.15
BSP4	Bacterial	5.4	3	3	1.15
BSP5	Bacterial	7.3	2	1	1.15
BSP6	Bacterial	3.9	3	3	1.15
BSP7	Bacterial	8.5	3	5	1.15, 1.75
BSP8*	Bacterial	8.5	2	2	1.6

SSP = sterilized sand pack, BSP = biotic or bacterial sand pack.

2.2. Brines and bacterial solutions

A sulphate-reducing bacterium strain *Oleidesulfovibrio alaskensis* G20 (DSM 17464) (14) was used as the model bacterium in this study. It is representative of sulphate-reduction reactions (11, 12) that may be encountered especially in anhydrite-containing reservoir rocks. A single strain was used to reduce the complexity of the study, but which still provided reliable information on hydrogenotrophic sulphate reduction reactions. *O.alaskensis* exhibits a growth range spanning pH 6.5 to 8.5, temperatures between 10°C – 45°C, and can thrive in NaCl concentrations ranging from 0–10% (w/v). The bacterium reaches its peak growth rate under optimal growth conditions in marine Postgate medium at 37°C, with a pH of 7.0 and 2.5% (w/v) NaCl, while utilizing lactate or acetate as a carbon source under anaerobic conditions (14). When grown on hydrogen, *Oleidesulfovibrio alaskensis* utilizes hydrogen as an electron donor and sulphate as an electron acceptor, resulting in the production of H_2S. For cultivation purposes, we employed a modified DSMZ growth medium solution (28) with reduced salt content as a base medium solution. The composition of the base medium solution is summarized in **Table S1** (**Supplementary Material**, available online) together with the nutrient solution and the bacteria solution brines used in the study. Pre-incubation of the bacterial solution was carried out at 37°C for a period of 3 days under anaerobic conditions, with a nitrogen gas head space. Following this three-day incubation, the culture was employed for injection into sand-pack columns for subsequent experiments.

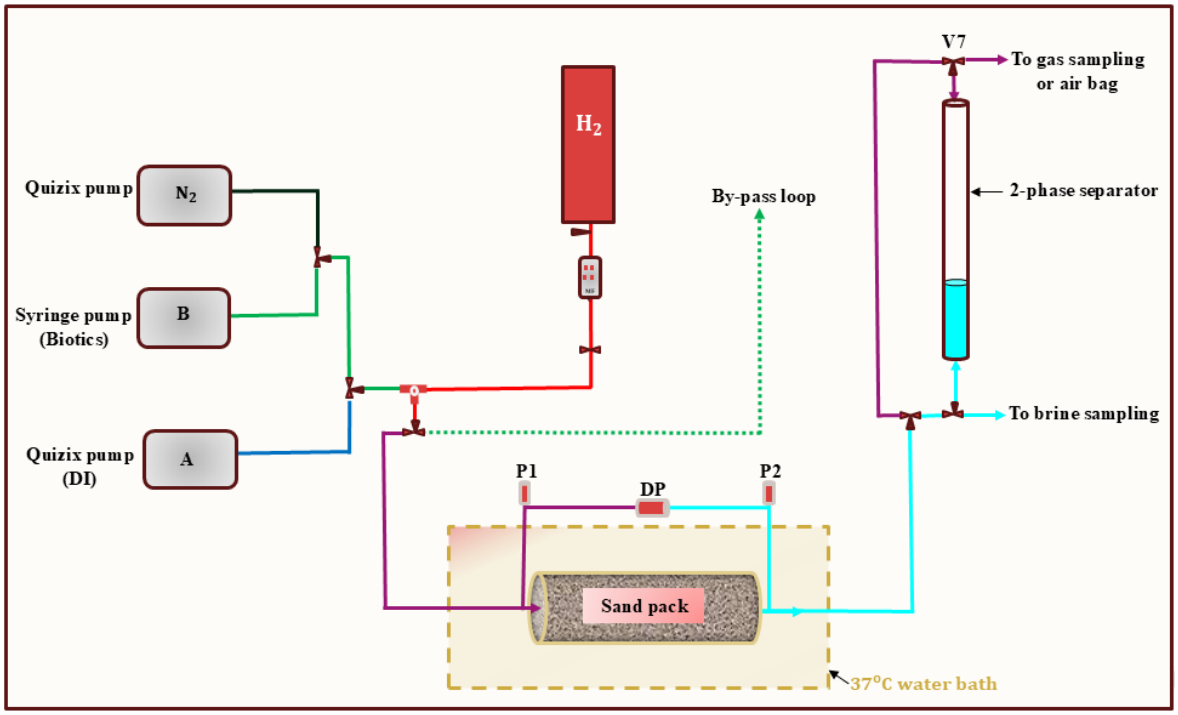

Figure 1: A schematic of the anoxic experimental set up used in the study. The anoxic environment was achieved by injecting degassed DI water and the base medium solution in combination with a network of valves. The dead volume in the network was minimized by using 1/16" peek flow tubing and connections. A hot water circulation pump ensured a constant temperature environment of 37°C around the sand pack, which was conducive for the growth of *Oleidesulfovibrio alaskensis* cells. A constant injection mass rate for hydrogen was possible with the use of the mass flow controller. Continuous pressure logging was limited to the sand pack inlet and outlet ends. Brine sampling was performed at the base of the 2-phase separator. Sampling was only performed at the end of the first drainage cycle or in situ brine at the end of each sand pack study.

3. EXPERIMENTAL PROCEDURE

3.1. Permeability measurements

Absolute permeability for each sand pack was measured with degassed deionized water and the base medium solution at 30 cm^3/hr and 45 cm^3/hr with the sand pack horizontally connected to the flow network (**Fig. 1**). The detailed procedure for permeability measurement can be found in the **Supplementary Material** (available online).

3.2. Anaerobic bacteria cultivation and growth

Two bacterial cultivation experiments were conducted on each test sand pack. One for bacterial growth and permeability tests and the second for microbial hydrogen consumption. For anaerobic bacterial growth, a solution mixture of 20% bacterial solution and 80% nutrient solution by volume with each solution sampled from its respective batch bottle was injected into the sand pack displacing the base medium solution. The solution mixture was opted to minimize bio-clogging at the sand pack inlet (16). Oxygen contamination during injection was monitored with Na-resazurin solution, which turned pink in case of contamination. The bypass loop was used to flush out the base medium solution before the sand pack. After injecting the bacterial-nutrient solution mixture, the sand pack system was shut-in for 5 days for bacteria adaptation and growth. During this time, the strain utilized lactate as both an electron donor and carbon source, leading to an increase in cell numbers. At the end of the shut-in period, the sand pack was flooded with the base medium solution at 30 cm^3/hr for permeability re-measurement. To prepare the porous medium for cyclic drainage tests and microbial hydrogen consumption, bacterial sand packs were re-flooded with a 100% bacterial solution containing starved cells with acetate as an electron donor, sampled from the same batch bottle as was used for the permeability tests. The system was shut-in for 2 hours to allow for equilibration, and subsequently it was drained using 100% H_2 gas, as detailed in the next section.

3.3. Extended drainage-storage tests

Hydrogen gas with a 99.999% (5.0) purity was used to displace the bacteria solution (BS) during immiscible drainage tests. Hydrogen was injected using a mass flow controller (F-200CV 002-AGD-11-V, ± 2% FS) with the outlet tubing from the sand pack connected to a transparent calibrated (1 cm = 0.24 ± 0.012 cm^3) two-phase separator. The bypass loop was used to flush out the BS in flow lines before hydrogen contacted the sand pack. Hydrogen was then injected at a rate of 60 cm^3/hour and the produced brine was collected in the separator. Injected hydrogen was not equilibrated with brine. The injection continued until 2–3 PVs after gas breakthrough. Brine production was recorded and the average gas saturation in the sand pack calculated by volumetric material balance. While hydrogen injection continued, the downstream valves of the sand pack were closed, and the system was pressurized to 1.15 bara to boost the hydrogen content within the system. The sand pack system was shut-in and the pressure across the sand pack monitored for 16–24 hours (storage period). A 0.3 cm^3 sample of the produced brine was collected at the separator for pH measurement. The ideal gas equation of state (**Eq. 5**) was applied to calculate hydrogen moles during storage based on the logged pressure readings. The microbial hydrogen consumption rate was empirically determined from the slope of the calculated moles versus the storage time curve.

$$\boldsymbol{n = \frac{RT}{PV} . 10^6} \tag{5}$$

In the above equation, $\boldsymbol{n}$ are the calculated moles in µmoles, $\boldsymbol{R}$ is the ideal gas law constant (8.314 J/Kelvin/mol), $\boldsymbol{T}$ is the temperature in Kelvin, $\boldsymbol{P}$ is pressure in Pascals, and $\boldsymbol{V}$ is the volume in m^3.

After the first storage period (16–21 hours), during which the pressure dropped close to the lower limit of the 2.5 bar ESI sensor, additional hydrogen was injected at 60 cm^3/hr to extend sand pack drainage from the previous cycle. Additional produced brine was recorded, and the hydrogen saturation was recalculated using a material balance approach. The sand pack system was repressurized to 1.15 bara and shut-in for the second storage period. The process was repeated for three consecutive drainage and storage cycles. Sand pack BSP7 was repressurized to 1.75 bara for an additional storage cycle to test the

effect of shut-in pressure on microbial hydrogen loss rate. The shut-in pressure for BSP8 in the first and second storage cycles was set to 1.6 bara. An in situ brine sample was extracted from all sand packs at the end of the last storage cycle to measure the residual brine pH. Drainage and storage cycles with the base medium solution as the initial fluid inside the sand pack created benchmark tests (sterilized cycles) for drainage tests with the bacterial solution (bacterial cycles). In bacterial cycles, hydrogen moles lost every hour were normalized against the hydrogen volume in the sand pack for comparison between cycles and across sand packs. The recorded value was subtracted from that obtained in the sterilized cycles (mechanical loss rates) to obtain the net moles lost to microbial consumption, as illustrated in **Equation 6**, and similar to the method used by Bagnoud et al (1). It was assumed that mechanical hydrogen losses due to permeation and dissolution were similar in both sterilized and bacterial sand packs, as the same experimental setup and sand pack holder were used.

$$\begin{aligned} &\boldsymbol{Net\ consumption\ rate} \\ &= \left|\left(\frac{\boldsymbol{Rate}}{\boldsymbol{Volume}}\right)\right|_{\boldsymbol{bacterialcase}} \\ &- \left|\left(\frac{\boldsymbol{Rate}}{\boldsymbol{Volume}}\right)\right|_{\boldsymbol{sterilizedcase}} \ \boldsymbol{\mu moles/(hour.ml)} \end{aligned} \tag{6}$$

The Rate is in µmoles/hour and Volume is the volume of hydrogen initially in place in cm^3 for each sand pack.

4. RESULTS

4.1. Permeability reduction due to bacterial growth on lactate

Permeability tests using a well grown bacterial solution provided indirect insight into the adaptation and growth mode of the bacterial cells and its effect on fluid flow. Bacteria cells were inoculated into the sand packs as suspensions in brine and hence occupied the same pore space as the brine. Biofilm growth with lactate as an electron donor was studied through the quantification of absolute permeability reduction after 5 days of bacterial cultivation. The relative loss from the initial sand pack permeabilities ranged between 3–11 ± 4%. For detailed results see **Figure S3** (**Supplementary Information**, available online).

4.2. Microbial hydrogen consumption

4.2.1. Total hydrogen losses

The sulphate-reducing *Oleidesulfovibrio alaskensis* was grown on hydrogen during consecutive storage periods in the bacterial sand packs and the hydrogen amount was monitored by continuous pressure logging for 16–21 hours. Microbial feeding constituted partial loss in the initial amount of hydrogen stored in respective sand packs. Other losses were related to mechanical processes assumed common to both sterile and bacterial tests such as hydrogen dissolution in brine and minor permeation in peek and flow connections. Such mechanical losses could be abiotic reactions with trace ions in solutions such as iron (iii). Representative results of the relative amount of hydrogen plotted against storage time in the four bacterial sand packs are shown in **Figure 2a-d**. The amount of hydrogen at selected time steps was normalized against the initial moles in a cycle. Total hydrogen loss in all sand packs, except for sterile cycles, was most significant in the first storage cycle amounting to percentage reductions ranging between 45–60%. There was no clear correlation between the declining trend in the amount of hydrogen and the hydrogen saturation at the beginning of the first cycles. Total losses on the second cycles were substantially lower than in the first cycles and accounted for 19–35% of the hydrogen amount at the beginning of the cycles. Losses in the third storage cycles were similar to the sterile tests except in a few tests (**Fig. 2c**).

4.2.2. Microbial hydrogen consumption rates in storage cycles

Total hydrogen loss in the bacterial sand packs followed a non-linear trend especially for the majority of the first and second storage cycles (**Fig. 2a-d**). However, on finer time intervals (<1 hour) the losses followed a relatively linear trend similar to the sterile cycles (**Fig. S7**, **Supplementary Material**, available online). Results of net microbial consumption rates in storage cycles plotted

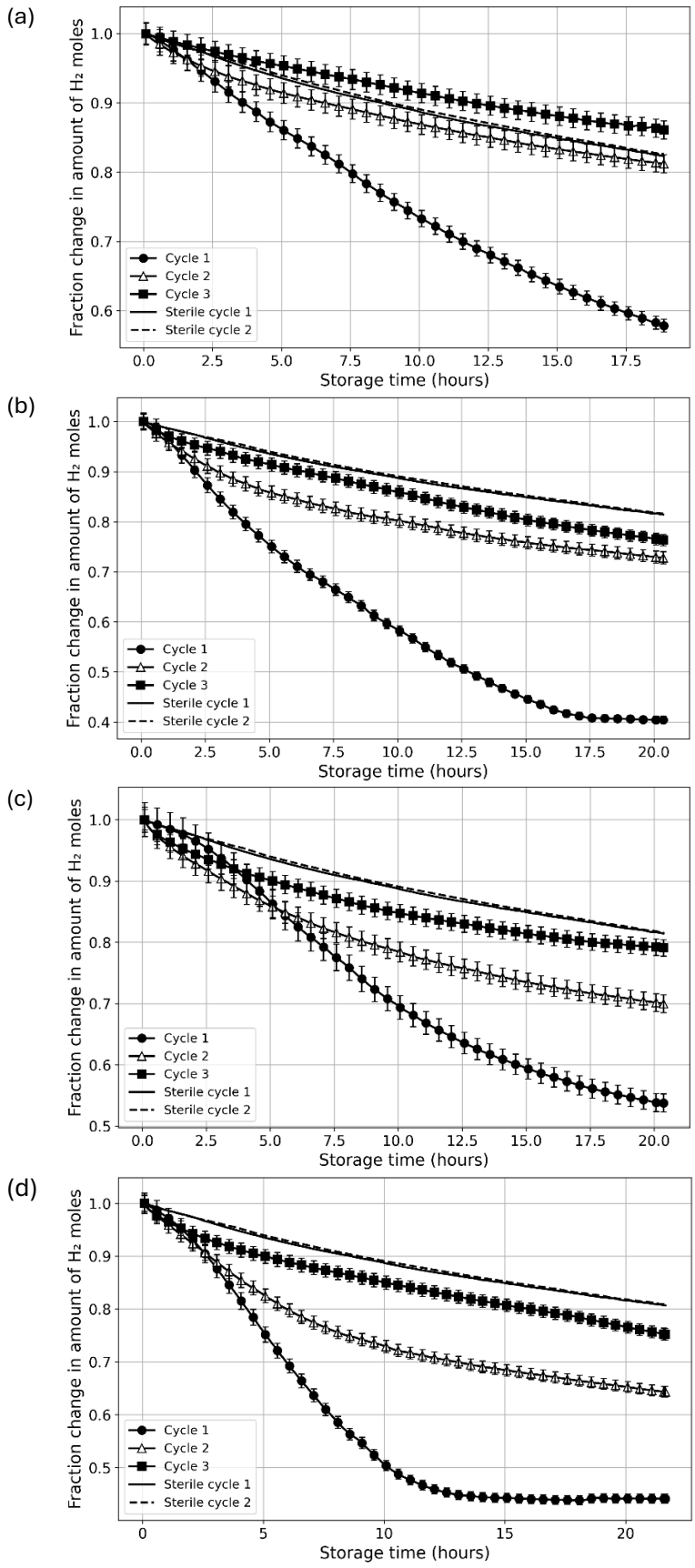

Figure 2: Quantitative evolution of the amount of hydrogen during shut-in periods (storage cycles) in four different sand packs (a: BSP2, b: BSP3, c: BSP6 and d: BSP7). Moles in each respective cycle were normalized against moles initially in place at the start of the cycle. The 1st cycles are plotted with solid circles, the 2nd cycles with triangles, and the 3rd cycles with squares. The sterile cycles are plotted as solid and broken lines without error bars. Mechanical losses in some of the 3rd cycles were lower than in the sterile cycles (**a**). The error bars account for small temperature variations (± 1°C), errors in volume measurements (± 0.024 cm^3), and pressure measurement uncertainty in mole calculations.

 https://doi.org/10.69631/ipj.v2i2nr72

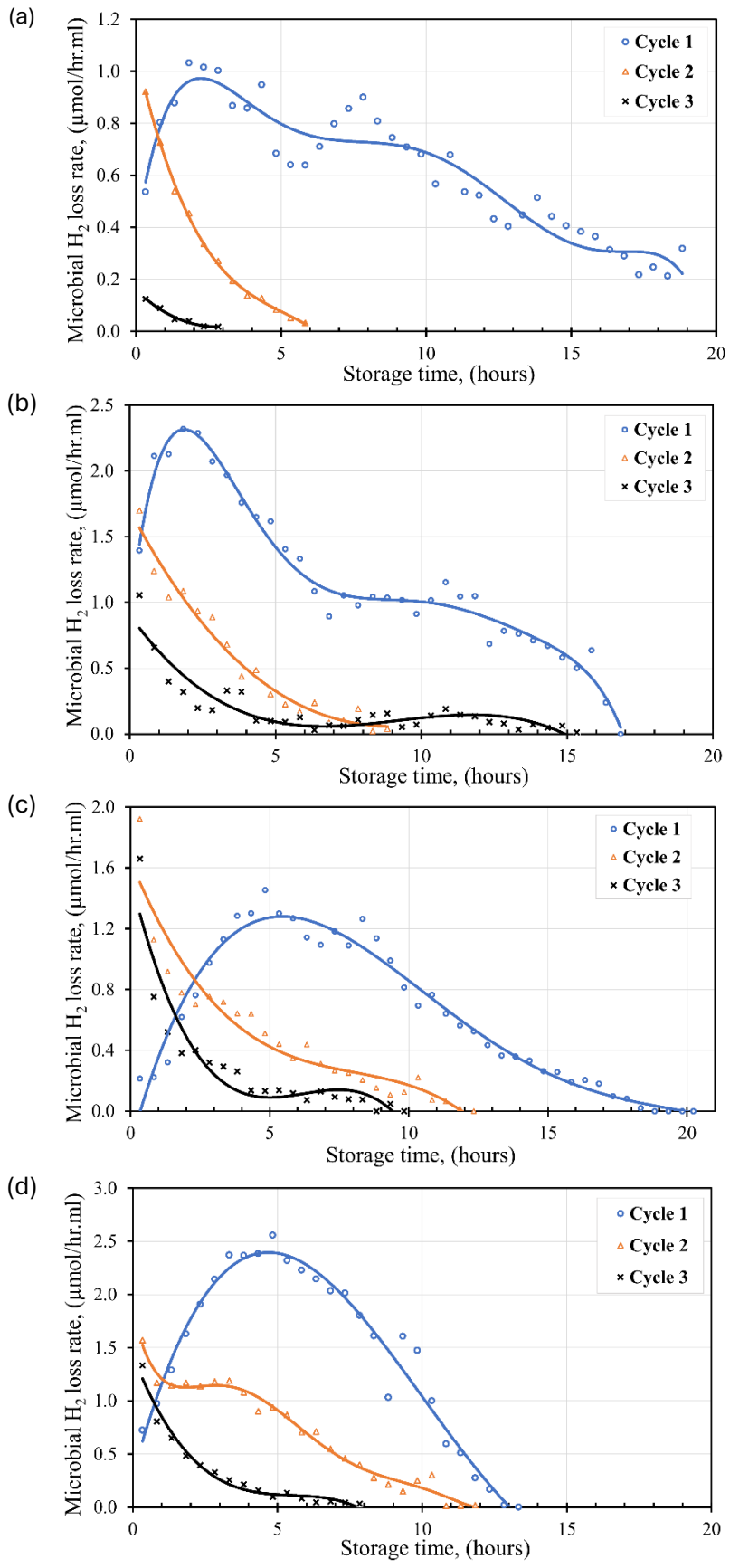

Figure 3: Microbial consumption rates at different times steps in three storage cycles for four different sand packs (**a:** BSP2, **b:** BSP3, **c:** BSP6 and **d:** BSP7). The scatters are the actual experimental data points whereas the solid curves are regressions fitted to the data points to capture the general trend in a cycle.

 https://doi.org/10.69631/ipj.v2i2nr72

against storage time in all sand packs are shown in **Figure 3a-d** and **Figure S8** (**Supplementary Material**, available online). As a general trend in the first storage cycles, hydrogen loss due to microbial consumption began immediately after shut-in with consumption rates steadily increasing to a maximum. The maximum consumption rates in this cycle ranged between 1.03 ± 0.03 – 2.55 ± 0.06 µmol/hr/ml in all sand packs and occurred within 2 to 5 hours from shut-in. After peaking, the rates monotonically decreased towards the zero rate with episodes of sustained consumption in some sand packs (**Fig. 3a, b**).

Consumption rates on the second storage cycles peaked immediately after shut-in and quickly decreased, reaching the zero-rate mark earlier than in the first cycles (**Fig. 3**). Maximum rates recorded in this cycle ranged between 0.32 ± 0.02 – 2.94 ± 0.07 µmol/hr/ml. Consumption rates in the third cycles followed a similar trend to that of the second cycles, but reached the zero-rate mark earlier than in the second cycles, except for BSP3 (**Fig. 3b**). Maximum rates in this cycle ranged between 0.73 ± 0.02 – 3.24 ± 0.07 µmol/hr/ml. In sand pack BSP7 (**Fig. 3b**), an extra storage cycle with shut-in pressure set to 1.75 bara instead of 1.15 bara did not result in a significant change in the microbial consumption rate (**Fig. 4a**), however it prolonged the consumption time before the rate reached zero. The prolonged consumption period resulted in a higher relative loss of 20% than in the previous cycle at 1.15 bara (8.3%). Increasing the pressure did not cause any observable change in the mechanical losses based on the sterile cycle losses at the same pressure **(Figure S7: Right**, **Supplementary Material**, available online). The observed hydrogen loss was thus associated with microbial consumption. The consumption rates and the trend between the first and second cycle did not change in the test with the initial pressure set to 1.6 bara BSP8 (**Fig. 4b**). Maximum rates in the first and second cycles were 1.72 ± 0.05 and 2.78 ± 0.05 µmol/hr/ml respectively.

4.2.3. Average consumption rates and endpoint pH

Results of the respective average consumptions rates in three storage cycles for the eight repeated experimental tests are shown in **Figure 5a**. The average rates and their uncertainties were calculated by considering net rates observed at respective time steps in a cycle. The average rates in the first

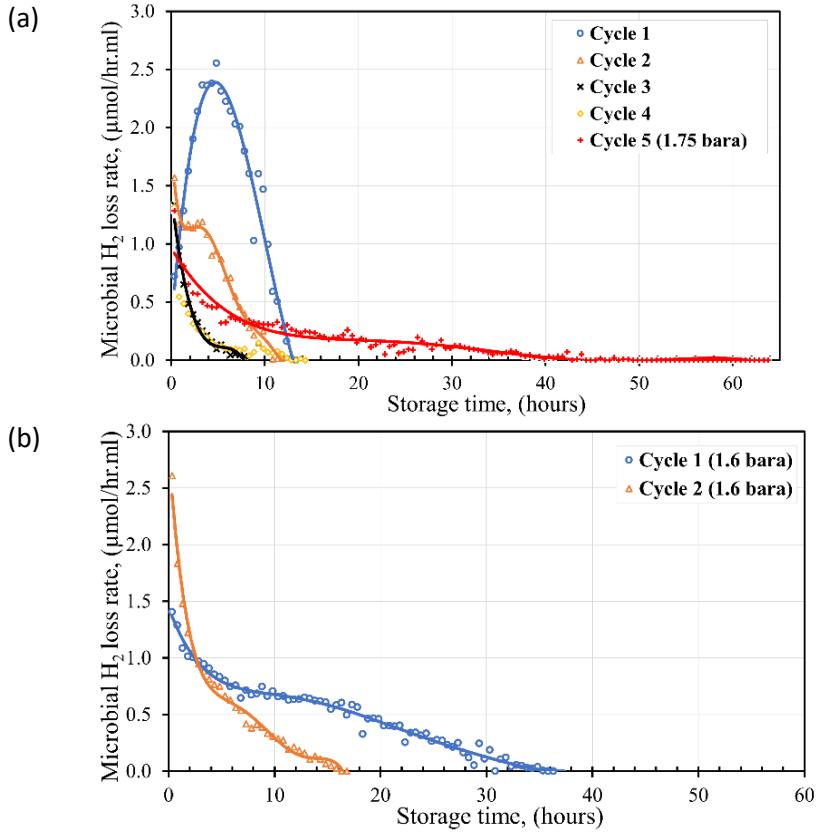

Figure 4: Pressure effect on microbial consumption rates in porous media. **a)** Consumption rates for BSP7 with a higher shut-in pressure (1.75 bara) than in the previous cycles (1.15 bara). **b)** Consumption rates in BSP8 with pressure in both the first and second cycles set to 1.6 bara was similar to the cycles set at 1.15 bara. The relative loss based on the area under each curve and the initial amounts in each cycle was 29% and 10% respectively. The volume for the initial gas in place was kept in the two cycles with no drainage cycle between them.

storage cycle were characterized by a period of buildup that peaked after about three hours and then steadily decreased towards zero after reaching the maximum. The maximum average consumption rate in the cycle was 1.26 ± 0.12 µmol/hr/ml. In relative terms, microbial hydrogen consumption in the first storage cycles caused a net percentage loss of 27.9 ± 12.4% (**Fig. 5b**) from the initial average amount of hydrogen (58 ± 19 µmoles). A relative loss equivalent to 16.2 ± 10.2 µmoles. Consumption in the second and third storage cycles was significantly lower with exponentially decreasing trends after shut-in. However, maximum rates of 1.53 ± 0.11 and 1.36 ± 0.01 µmol/hr/ml in the second and third cycles respectively were distinctively higher than in the first cycle. The net percentage loss was also significantly lower at 10.2 ± 5.3% (6.9 ± 4.5 µmoles) for the second cycle and 5.6 ± 3.4% (3.8 ± 2.4 µmoles) for the third cycle. The average in-situ brine pH at the end of the third storage cycle was 8.4 ± 0.2 for the bacterial tests and 7.3 for the sterile tests. **Table 2** summarizes the start and endpoint brine pH for all sand packs. The consumption rates were

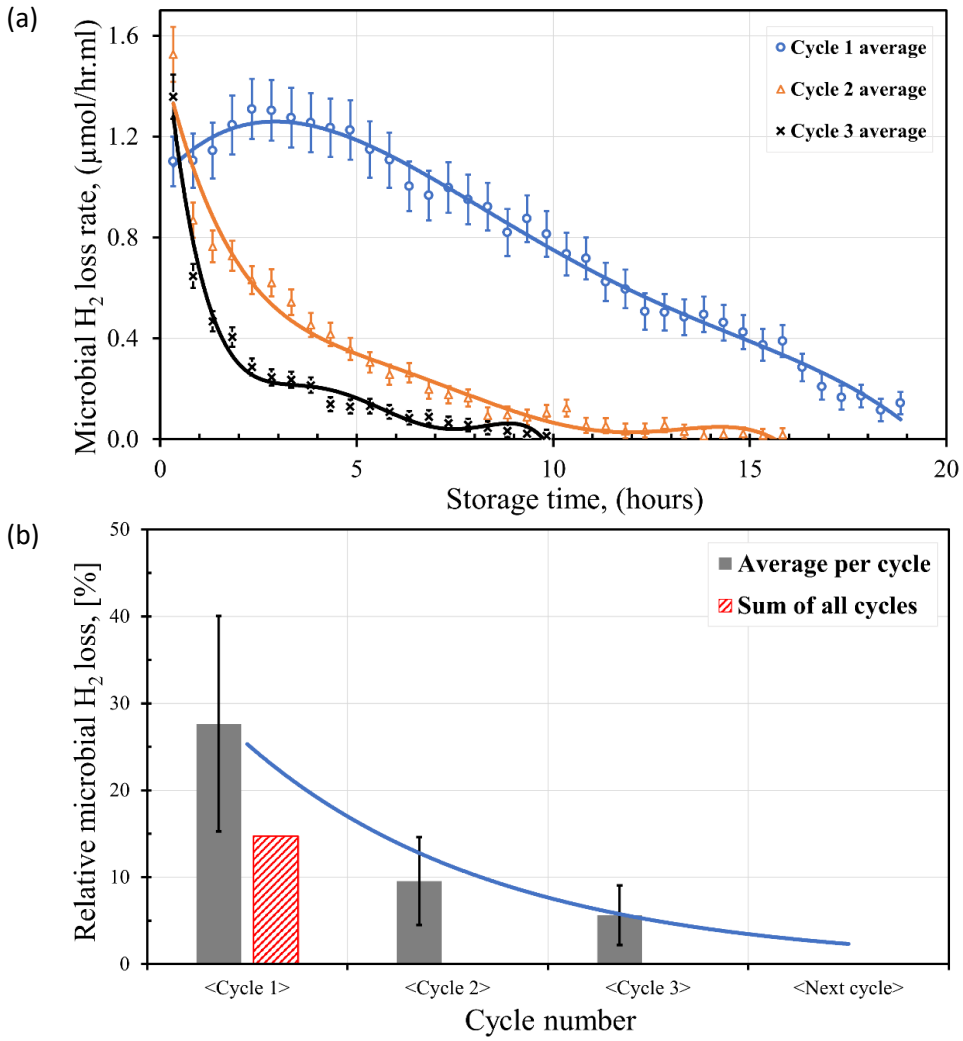

Figure 5: a) Average microbial consumption rates in three storage cycles based on eight experimental repetitions. The error bars are the standard deviations in the averaged rates at the selected time steps. Microbial hydrogen consumption was most dominant in the first storage cycle, and continuously decreased in the second and third storage cycles. **b)** Average relative loss in the amount of hydrogen in three storage cycles due to microbial consumption. The bar with stripes is for the cumulative loss in the three cycles with respect to the total amount of hydrogen stored. Microbial activity exponentially decreased with storage cycle number based on the regressed blue curve fitted to the average relative losses in the three cycles.

 https://doi.org/10.69631/ipj.v2i2nr72

compared with reported literature rates commonly observed in batch bottle tests. The rates in the porous medium were found to be one to two orders of magnitude higher than in batch bottles, and the difference was associated with the large specific surface area in porous media that catalyzes microbial-driven reactions.

Table 2: Summary of the of the experimental results across all the sand packs. S_{gi} is the average gas saturation at the start of a storage cycle. The slight pH increase in the sterilized case was attributed to measurement errors or abiotic reactions in the system. Only hydrogen loss attributed to microbial consumption has been summarized in the table.

Sand Pack ID	Sum of moles in all cycles (µmol)	Cum. loss for all cycles (%)	Loss 1st cycle/ Cum. Loss (%)	Max. CR (1st cycle) (µmol/hr/ml)	Initial pH	End pH	S_{gi} (1st cycle) (%)	S_{gi} (2nd cycle) (%)	S_{gi} (3rd cycle) (%)
BSP1	167	7	61	1.03	7.6	8.0	29	34	37
BSP2	208	10	88	1.03	7.5	8.5	44	44	48
BSP3	209	20	69	2.31	7.4	8.6	42	44	50
BSP4	175	9	31	2.36	7.5	8.2	30	35	39
BSP5	32	-	100	1.87	-	-	11	13*	-
BSP6	158	11	45	1.45	7.4	8.6	18	30	41
BSP7	202	18	57	2.56	7.5	8.5	34	45	50
BSP8*	196	19	69	1.72	7.3	8.3	45	-	-
Avg	194	15	61	1.26	7.5	8.4	30	35	44
SSP1	-	-	-	-	-	-	13	14	14
SSP2	-	-	-	-	7.2	7.3	34	34	35
SSP3	-	-	-	-	-	-	24	24	24

Avg = average; CR = Consumption rate; Cum. = cumulative; Max. = maximum; SSP = sterilized sand pack, BSP = biotic or bacterial sand pack.

4.2.4. Average hydrogen-in-place saturation after drainage cycles

The microbial effect on the porous media storage capacity was analyzed by evaluating the magnitude of hydrogen gas saturation at the end of the drainage cycles. Average hydrogen saturations were evaluated based on material balance calculations during steady state drainage after gas breakthrough (**Fig. S4** in the **Supplementary Material**, available online). Saturation results of the hydrogen gas in-place at the end of each drainage cycle are summarized in **Table 2**. In the three sterilized cycles, the gas saturation remained relatively constant throughout all the three drainage cycles, with only one sand pack showing a 1 ± 1.4% increase. However, in the bacterial sand packs, the gas in-place saturation significantly improved between the first and third drainage cycles. The increments ranged between 4–24 ± 1.4%. The error percentage was attributed to the measurement uncertainty of the two-phase separator. No clear correlation was observed between the saturation in the first non-sterile cycle and the subsequent improvement. However, the largest increment of 24% was recorded in the sand packs with the second lowest saturation (18% after the first cycle).

5. DISCUSSION

5.1. Permeability reduction.

Bacterial growth under optimal and stress conditions can cause biofilms to develop as a result of excess energy from cell respiration or as a defense mechanism respectively (34). In our study, growth was anticipated to be optimal during the first one to two days, followed by a decline as lactate levels decreased due to its limited initial concentration (**Table S1** in the **Supplementary Material**,

available online). The permeabilities were expected to reduce since *Oleidesulfovibrio alaskensis* is known to form dense biofilms under optimal growth conditions (14, 44), and the sand grains were anticipated to be ideal attachment surfaces. However, the extent of permeability loss, (3–11 ± 4%), suggests that biofilm accumulation was on a scale that could not significantly affect fluid flow. It was then inferred that either most of the cells adapted and grew as suspensions in brine (planktonic mode (21, 34, 46) that could not significantly alter the brine viscosity, or that the accumulated biofilms were permeable to the same extent as the sand packs. The presence of biofilm development was consistent with previous sand pack studies (7, 35, 36, 39), but to a lesser extent in regard to permeability damage. Relevant to our study, the observed microbial growth and adaptation mode implied the following: **1:** The sand pack environment was conducive for anaerobic bacteria cells to adapt and grow in a way similar to batch bottle tests; **2:** Initial sand pack pore volume did not significantly change after bacteria growth; and **3:** Ideal growth conditions may not always result in biofilm development that has negative implications on the reservoir quality in relation to permeability and porosity.

5.2. Temporal microbial hydrogen consumption rates

Using relatively identical sand packs as porous media analogues, we experimentally studied and quantified the microbial hydrogen consumption rates of the microbial sulphate reducer *Oleidesulfovibrio alaskensis,* previously described as capable of utilizing hydrogen as an electron donor in the presence of sulphate and a carbon source (14, 26, 44). The consumption rates were measured in three storage cycles. A strong correlation between consumption trends in each cycle across all sand packs was observed, with consumption being the highest in all first cycles and then exponentially decreasing in subsequent cycles. Consumption rates in the first storage cycles (**Fig. 3**) followed a typical growth curve for microbes that are in excess of substrate supply (17, 21). The rates began relatively low and built up to a global maximum, where, for most cycles was relatively sustained for 2–5 hours before declining to a minimum either monotonically or in a step-like manner. Despite the low initial rates, they were non-zero, indicating immediate hydrogen consumption by the bacteria. The prompt consumption could be explained by the minimal shear stress imposed on bacteria cells during hydrogen injection (22) and depletion of lactate in solution during cultivation causing the cells to starve. The rise to a maximum value indicated that bacterial cells increasingly consumed hydrogen as more hydrogen dissolved in the brine, despite its low solubility under the experimental conditions (0.00014 g/kgw) (5, 6, 18). Based on the average initial pH of 7.4 in the first cycle and the optimal temperature sustained at 37°C, microbes consumed dissolved hydrogen (7, 11, 13, 40) especially at the free hydrogen-brine contact points. However, given the relatively high sand pack permeabilities (over 3 Darcy, **Table 1**), dissolved hydrogen was expected to easily diffuse between sand pack pores (8, 17, 47) and eventually be consumed by the cells, sitting further away from the brine-gas contact line. Microbial hydrogen consumption was thus present throughout the pore space for most of the first storage cycle. Although *Oleidesulfovibrio alaskensis* cells are known biofilm-forming microbes (14, 44), it was assumed that during the first storage cycles, individual cells initially stayed suspended in the brine since they were starved prior to inoculation. It is known that starved bacteria cells prefer to live in a planktonic mode in search of food, rather than forming cell clusters or using energy to produce EPS (extracellular polymeric substance) molecules necessary for biofilms (34). Therefore, mobility for food was at its best in the first cycles, and hydrogen dissolution and diffusion in brine was at its highest since injected hydrogen was not equilibrated with brine. Based on a pseudo steady state loss rate of 0.41 ± 0.09 µmol/hr/ml in sterile tests (**Figure S7 (left)** in the **Supplementary Material**, available online), hydrogen dissolution in brine without bacteria activity was estimated at 2.9–3.6 µmoles/ml(H_2) for a storage period of 16 to 21 hours. The dissolution loss was consistent with previous experimental and numerical studies (1, 5, 6, 18). Hydrogen dissolution rates in the non-sterile cycles were expected to be similar to the sterile cycles given that brines were of identical salinity (5) and at the same temperature and pressure. As microbial hydrogen consumption progressed, it was expected that more free hydrogen dissolved in brine prompting additional consumption loss. The decline in average consumption rates after the peak rate in the first cycle

(**Fig. 5a**) could be associated with the physical-chemical conditions inside the sand packs, especially brine pH. It is known that *Oleidesulfovibrio alaskensis* cells are sensitive to pH and become inactive at an alkaline pH of 8.5-9.0 (14, 26, 44). Previous batch (11, 13, 40) and microfluidic (21) studies with other anaerobic sulphate reducing strains have shown this pH dependence for microbial hydrogen oxidation. As consumption proceeds, the brine pH increases since anaerobic sulphate reduction with hydrogen as an electron source is a proton consuming process (26) (**Eq. 1**). However, partial dissociation of the reaction by-products (H_2S and HS^- shown in **Eq. 2** and **Eq. 3**) in brine releases protons as the pH changes, but the concentrations are low and thus counteract the proton-consuming process (4, 13, 19). The start and end pH values in all bacterial sand packs are summarized in **Table 2** together with the pH of the sterile case. We suggest that the net hydrogen consumption began to decline during the first cycle as the pH increased over storage time, eventually leading to an end of the consumption. Subsequent hydrogen loss was likely attributable solely to mechanical losses (**Fig. 2b, d**). It is known that harsh brine pH conditions result in cell-to-cell communication, leading bacteria to form biofilm clusters as an adaptive and protective response (42). The in situ brine endpoint pH of 8.4 ± 0.2 after the second (BSP8) and third cycles fell within the hostile range for *Oleidesulfovibrio alaskensis* cells. Biofilm formation was microscopically confirmed around the sand grains (**Figure S4** in the **Supplementary Material**, available online).

Biofilms were expected to develop on grains at the hydrogen-brine contact area before spreading out to the rest of the sand pack for two reasons: **1)** Microbial activity was highest at the interface due to excess substrate (hydrogen) supply, and **2)** High local hydrogen consumption resulted in a swift increase in pH making brine hostile for bacteria cells. The nature of biofilm development increased heterogeneity in the sand packs. Biofilms are known to make a relatively homogenous porous medium in terms of pore size and structure, becoming increasingly heterogenous which adversely affects mass transfer (8, 9, 33, 34). During the storage cycles, molecular diffusion was the main form of hydrogen, nutrient and waste transport for microbes in biofilm clusters. This implied that the complex pore structures increased the mean free path for diffusion (8, 9, 17, 47) in addition to enhancing hydrogen adsorption at the pore walls (25, 30, 47). The two processes resulted in a substantial reduction in the hydrogen loss rates. Eventually hydrogen losses resulting from both microbial activity and mechanical losses increasingly decreased as seen at the tail end for **Figure 2b, d**.

At the start of the second storage cycle (**Fig. 3a-d**), microbial consumption resumed despite the ultimate zero consumption rates recorded in most of the first cycle. The rejuvenated activity could be explained by three processes: **1)** Flushing out of potential toxic waste by injected hydrogen during drainage at end of the first storage cycle; **2)** Cell detachment from biofilms and bacteria clusters. Detaching cells are known to be more metabolically active than cells in biofilm communities (34, 37); and **3)** Dispersive fluid mixing during drainage introduced new contact areas with potential for additional hydrogen consumption. All three processes caused immediate effects that resulted in maximum consumption rates for some sand packs which were higher than in the first cycle. However, the improved environmental change was short-lived, and eventually consumption rapidly ceased thereafter. The same processes occurred in the third storage cycle, but with less microbial loss than in the second cycle. Brine composition calculations confirmed that both sulphate and acetate remained available in solution throughout the three storage cycles, indicating that neither substrate was limiting consumption (**Table S2** in the **Supplementary Material**, available online). Increasing shut-in pressure to 1.75 and 1.6 bara was expected to increase the hydrogen dissolution rate, but not the overall dissolved amount due to a small pressure margin (5). However, a significantly higher pressure, (reservoir conditions of above 50 bar) would still result in a minimal increase in dissolved hydrogen due to the relatively small variation in hydrogen solubility in brine across different pressures. In this study, no substantial change in the consumption rates was observed because of increased dissolution rates (**Fig. 4**). It could be that the positive effect of hydrogen dissolution in brine was cancelled out by low diffusion rates as the mean free path for dissolved molecules was reduced due to increased molecular collisions (25, 30) and complex biofilm

structures (8, 47). Overall, microbial hydrogen loss was highest in the first storge cycle and exponentially decreased in the second and third cycles (**Fig. 5b**). A slight increase in shut-in pressure did not change the consumption rates and relative hydrogen losses between cycles.

Under the experimental conditions, and based on the peak hydrogen consumption rates observed during the first cycles, we calculated the amount of dissolved hydrogen that *Oleidesulfovibrio alaskensis* cells could consume before the pH reaches a threshold beyond which further hydrogen consumption becomes unfavorable. This would be around 0.016 ± 0.009 moles/L (brine) for a three-cycle storage scenario. The threshold pH was fixed at 8.4 ± 0.2. However, it is important to point out that this calculation was based on hydrogen dissolution in brine with salinity of ≈3.5%. In formation brines with salinities between 10-30%, we would expect the hydrogen dissolution rate to be lower (5), and hence the consumption period might be longer at lower rates. The calculations were also based on the initial brine pH of 7.5, and yet formation brine pH dependent on the brine composition could be more or less alkaline than 7.5.

5.3. Effect of brine-gas interface area on microbial hydrogen consumption

An additional control parameter coupled to microbial consumption rate is the hydrogen-brine interface area boosted by the specific surface area (SSA) in a porous medium. The SSA in a porous media is a few orders of magnitude higher than in batch bottles for the same volume space. In the current study, the SSA of 76 cm^2/cm^3 for a fully brine-saturated sand pack was 3 orders of magnitude higher than the SSA calculated for the serum bottle with a 42.4 mm inner diameter (0.24 cm^2 /cm^3) used by Thaysen et al (40), Dopffel et al (13) and Dohrmann et al (11). We observed that the SSA in sand packs correlated positively with a higher microbial consumption for every unit of hydrogen, as shown in **Figure 6**, in comparison with the batch tests. Increasing the specific interface area by two orders of magnitude from the batch tests to sand packs resulted in a two-order

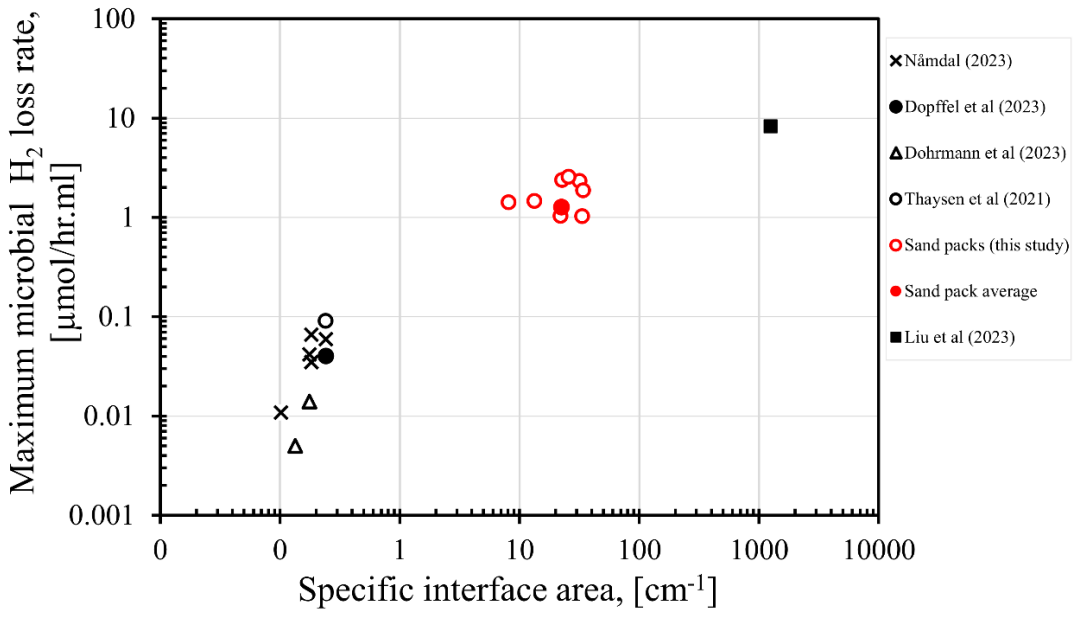

Figure 6: Comparison of anerobic microbial hydrogen consumption rates from literature batch tests and the current sand pack measurements (red scatters). The differences in initial molar concentration for literature tests was corrected for by normalizing molar concentrations in the headspaces against the smallest molar concentration in the smallest head space volume. The difference in specific interfacial areas between sand packs originates from the initial gas-in-place saturation levels during the first storage cycle. The solid black square shows the rate from a microfluidic study by Liu et al (21) with *D. retbaense* as a sulfate reducer, and is similar to Dopffel et al (13). Thaysen et al (40) and Dohrmann et al (11) used formation brines containing different strains of sulphate reducers with a focus on *Desulfovibrio* G11 (40). Whereas Nåmdal et al (24) used *Oleidesulfovibrio alaskensis,* as done in this study.

magnitude increase in the consumption rate. On the contrary, the rates in the micromodel sample (black square, **Fig. 6**) were comparable with the sand pack rates despite the SSA being two orders of magnitude higher than the micro model. The increase in rates with a specific area was consistent with previous studies (11, 24). However, for most of the batch tests, the reported rates were within the same range (11, 13, 24, 40) (0.01 - 0.1 µmol/hr/ml) and were significantly lower than in sand packs (**Fig. 6**). It implied that the larger SSA in sand packs catalyzed hydrogen dissolution in brine. This process increased hydrogen availability to the microbes, thereby accelerating their consumption. Therefore, the difference in the microbial hydrogen consumption rates reported in the current study from most of the batch studies (11, 13, 40) could be explained by the large interface areas provided by the sand grains. As the reaction accelerated, the brine pH increased more rapidly than in the batch tests (13), ultimately leading to a faster slowdown in microbial activity. This partly explains the rapid (within hours) pH increase observed in the sand packs, and the corresponding decrease in hydrogen consumption rate compared to previous studies (11, 13). In the batch tests conducted by Dopffel et al (13), a one-unit increase in pH was recorded over the course of a month from the start of the experiment. The reported higher consumption rates observed in this study compared to batch tests may indicate a more rapid pH increase, which eventually limits microbial activity in relation to hydrogenotrophic sulphate reduction. The process could be vital in reducing microbial risk for underground hydrogen storage.

5.4. Microbial effect on storage capacity and endpoint relative permeability

The impact of bacterial cells on fluid flow and distribution during drainage and storage was evident through observed sequential increments on the average hydrogen saturation between drainage cycles. In sterile sand packs, the average gas saturation in all three drainage cycles remained relatively constant. This implied that brine displacement was identical with injected hydrogen following the same flow paths between cycles. The early gas breakthrough times indicated that gravity override and gas fingering dominated the fluid displacement in a manner similar to the experimental studies by Boon et al (3) and Lysyy et al (23). For the bacterial sand packs, a combination of bacteria and biofilms controlled fluid flow. The saturations in the first drainage cycles were comparable to the sterile cycles (**Table 2**). It can hence be assumed that fluid displacement was identical. However, increments in the average gas saturation on the second and third cycles could be inferred to the biofilm effect on fluid flow. It is known that the accumulation of biofilms in a porous medium affects fluid flow (7, 32, 39). Previous studies have shown that biofilm growth in a porous medium starts in established flow channels and from there spreads out to other areas of the medium (17, 32, 33). It was likely that new flow paths were established in the second and third drainage cycles because of biofilm accumulation in the previous flow channels. Upon hydrogen re-injection, hydrogen gas contacted new areas of the sand pack displacing additional brine. The stage of biofilm growth also determined the style of fluid displacement (33). In the early biofilm growth stage, fluid displacement is piston-like, and the injected phase contacts more of the pore space (17, 33). However, well-developed biofilms could result in established flow channels (17), which in turn result in poor areal sweep during subsequent injections. It was difficult to characterize the biofilm growth stage in situ and its impact on fluid displacement with our experimental design. In future experiments, we plan to use high resolution MRI imaging to visualize and quantify biofilm dynamics and its effect on fluid displacement.

In addition, it was likely that the improved gas saturation between drainage cycles could be partly related to an improved hydrogen sweep efficiency due to reduction in the water wetness of the sand grains (21). Hydrogen adsorption on the grains and in the interstitial voids of the biofilms could create continuous thin gas films connecting multiple pores (25, 30). This could reduce the water wetness of the sand grains and average entry capillary pressure for hydrogen. Therefore, injected hydrogen invaded and displaced more brine from the pores. In addition, the biofilms and cell membranes of halophilic mesophiles are partially composed of polar protein molecules (26, 40), which may alter the water wetness of sand grains, shifting them toward a more neutrally wet state.

Wettability alteration to a less water wet state due microbial hydrogen consumption was previously demonstrated by Liu et al (21) with a quartz micromodel sample. It was observed that the average contact angle increased from 41° to 96° after a shut-in period of 24 hours. The sand grains in our study were mostly composed of quartz, and the storage periods were within the same experimental window. We therefore propose that both wettability alteration and increased sweep due to cell attachment and biofilm development may enhance brine displacement in the non-sterile drainage cycles. The extent to which this wettability alteration would occur in actual reservoir conditions, where mineralogy is complex and aged, remains an open question for future investigation.

The average gas saturation in a reservoir has direct implications for UHS efficiency as it dictates how much of the pore space can be utilized for hydrogen storage. Our study suggests that higher volumes of hydrogen could potentially be stored in rocks containing native bacteria in the formation brine, compared to those with sterilized brine. Even though we have only looked at one bacterial strain, it is known that sulfate reducing microbes are among the likely hydrogen consumers to be encountered in aquifers or depleted oil and gas reservoirs (11, 12, 19, 40). Our experiments indicate that even though microbial hydrogen consumption is significant, especially in the first storage cycle, a higher average gas saturation and reduced hydrogen consumption follow in subsequent storage cycles in low-buffered systems. However, it is important to highlight that further tests need to be studied with different microbes, formation brines, and on actual reservoir cores or at least representative outcrop cores, where the pH increase might be buffered by secondary minerals or dissolved carbonates.

5.5. Implications for UHS in porous media

In the context of UHS, the accelerated microbial consumption rates observed in our study can be viewed as both negative and positive. On one hand, under ideal reservoir physical-chemical conditions, microbial hydrogen consumption by sulphate reduction could significantly cause hydrogen loss and hence reduce the hydrogen recovery factor. Also, H_2S as a toxic byproduct could substantially alter hydrogen purity if some of formed H_2S is produced with the hydrogen. In addition, the corrosive effect of H_2S on well bores and surface facilities as a result of hydrogenotrophic sulphate reduction requires further study. However, the observed higher consumption rates compared to batch bottles, also lead to a faster increase in brine pH, which will limit the total hydrogen consumption. Large interfaces in porous media might accelerate the pH increase, which over time could reduce the overall microbial risks. The reduced activity with storage cycle numbers also implies that the purity of the working gas will be closer to the injected gas after a certain number of cycles. This, however, will depend on the overall pH buffer potential of the brine and the reservoir itself. In our study, ideal conditions were created for anaerobic sulphate reducing bacteria to grow in sand packs, inoculating with a high cell number solution. The sulphate ion concentration and a carbon source were in excess in all storage cycles and therefore high concentrations of hydrogen could potentially be lost to microbial consumption. In natural reservoirs, sulfate concentrations are often limited to micro- or nanomolar levels per liter of formation brine (11, 13, 40), which would also constrain hydrogenotrophic sulfate reduction. In addition, there is a need for caution during cyclic operations to prevent contamination of reservoir brine with sulfate-reducing bacteria or nutrient ions that could stimulate the activity of existing microbial communities. Regular monitoring of both the recovered hydrogen and the reservoir brine composition may be necessary to ensure that microbial risks are effectively controlled or mitigated. Further empirical studies are required to develop comprehensive datasets that can provide reliable input for field-scale simulations of cyclic operations. While our study focused on a sulfate-reducing microorganism, it is important to note that other microbial strains—such as methanogens and acetogens—may also be present at geological storage sites and contribute to hydrogen loss.

6. CONCLUSIONS AND OUTLOOK

We developed an experimental sand pack column set-up to conduct anaerobic microbial hydrogen consumption tests in porous media using the known hydrogen consumer and sulphate reducer *Oleidesulfovibrio alaskensis*. Growth tests through absolute permeability analysis showed a relatively low permeability reduction (3–11 ± 4% from the initial permeability) caused by low cell plugging and low biofilm formation. Observed hydrogen consumption rates exponentially decreased after the first storage cycle caused by a significant pH increase. The end-point average pH of 8.4 made the brine solution hostile for the bacteria cells. Compared to literature-reported batch tests, the hydrogen consumption rates in the sand packs were higher, likely due to the larger specific interfacial area that accelerated microbial activity. We also observed that microbial presence could have a positive effect on the porous media storage capacity by changing the wettability of the sand surface. Additional datasets are needed to quantify and fully understand the risk of microbial hydrogen consumption at both the lab scale and the natural setting. In this study, clean sand was used. Future studies should consider reservoir rock samples with more representative mineralogical compositions to better reflect in situ conditions. Other microbial strains prevalent in potential reservoir rocks should also be studied both individually and in combination to help close the knowledge gap regarding microbial hydrogen consumption.

STATEMENTS AND DECLARATIONS

Supplementary Material

The Supplementary Material for this paper is available online alongside the article or can be accessed directly via the following link.

Acknowledgements

The authors acknowledge funding from the Centre of Sustainable Subsurface Resources (CSSR), grant nr. 331841, supported by the Research Council of Norway, research partners NORCE Norwegian Research Centre and the University of Bergen, and user partners Equinor ASA, Harbor Energy, Sumitomo Corporation, Earth Science Analytics, GCE Ocean Technology, and SLB Scandinavia. Additional acknowledgement for funding from Hydrogen Storage in Subsurface Porous Media-Enabling Transition to Net-Zero Society (HyPE), project nr. 325457)

Author Contributions

The manuscript was compiled with contributions from all the listed authors. **Raymond Mushabe:** Conceptualization, set-up design and construction, data collection and analysis, and writing the original draft. **Na Liu:** Supervision, conceptualization, data collection and analysis, writing and reviewing, microbial expertise. **Geir Ersland**: Supervision, writing and reviewing. **Nicole Dopffel:** Supervision, writing and reviewing, microbial expertise. **Martin A. Fernø**, funding acquisition, writing and reviewing.

Conflicts of Interest

The authors declare to the best of their knowledge that they have no known financial and selfish personal interests that could have influenced the work that has been done in this study.

Data, Code & Protocol Availability

Raw data can be provided upon request.

ORCID IDs

Raymond Mushabe https://orcid.org/0000-0002-1263-2449
Na Liu https://orcid.org/0000-0002-0016-6292
Nicole Dopffel https://orcid.org/0000-0003-0020-9579
Geir Ersland https://orcid.org/0000-0002-5805-3573
Martin A. Fernø https://orcid.org/0000-0002-5744-0825

REFERENCES

1. Bagnoud, A., Leupin, O., Schwyn, B., & Bernier-Latmani, R. (2016). Rates of microbial hydrogen oxidation and sulfate reduction in Opalinus Clay rock. *Applied Geochemistry*, 72, 42–50. https://doi.org/10.1016/j.apgeochem.2016.06.011
2. Barison, E., Donda, F., Merson, B., Le Gallo, Y., & Réveillère, A. (2023). An insight into underground hydrogen storage in italy. *Sustainability*, 15(8), 6886. https://doi.org/10.3390/su15086886
3. Boon, M., & Hajibeygi, H. (2022). Experimental characterization of H_2/water multiphase flow in heterogeneous sandstone rock at the core scale relevant for underground hydrogen storage (UHS). *Scientific Reports*, 12(1), 14604. https://doi.org/10.1038/s41598-022-18759-8
4. Carroll, J. J., & Mather, A. E. (1989). The solubility of hydrogen sulphide in water from 0 to 90°C and pressures to 1 MPa. *Geochimica et Cosmochimica Acta*, 53(6), 1163–1170. https://doi.org/10.1016/0016-7037(89)90053-7
5. Chabab, S., Théveneau, P., Coquelet, C., Corvisier, J., & Paricaud, P. (2020). Measurements and predictive models of high-pressure H_2 solubility in brine (H_2O+NaCl) for underground hydrogen storage application. *International Journal of Hydrogen Energy*, 45(56), 32206–32220. https://doi.org/10.1016/j.ijhydene.2020.08.192
6. Crozier, T. E., & Yamamoto, S. (1974). Solubility of hydrogen in water, sea water, and sodium chloride solutions. *Journal of Chemical & Engineering Data*, 19(3), 242–244. https://doi.org/10.1021/je60062a007
7. Cunningham, A. B., Characklis, W. G., Abedeen, F., & Crawford, D. (1991). Influence of biofilm accumulation on porous media hydrodynamics. *Environmental Science & Technology*, 25(7), 1305–1311. https://doi.org/10.1021/es00019a013
8. De Beer, D., Stoodley, P., & Lewandowski, Z. (1997). Measurement of local diffusion coefficients in biofilms by microinjection and confocal microscopy. *Biotechnology and Bioengineering*, 53(2), 151–158. https://doi.org/10.1002/(SICI)1097-0290(19970120)53:2<151::AID-BIT4>3.0.CO;2-N
9. De Beer, D., Stoodley, P., Roe, F., & Lewandowski, Z. (1994). Effects of biofilm structures on oxygen distribution and mass transport. *Biotechnology and Bioengineering*, 43(11), 1131–1138. https://doi.org/10.1002/bit.260431118
10. Diao, C., Ye, W., Yan, J., Hao, T., Huang, L., et al. (2023). Application of microbial sulfate-reduction process for sulfate-laden wastewater treatment: A review. *Journal of Water Process Engineering*, 52, 103537. https://doi.org/10.1016/j.jwpe.2023.103537
11. Dohrmann, A. B., & Krüger, M. (2023). Microbial H_2 consumption by a formation fluid from a natural gas field at high-pressure conditions relevant for underground H_2 storage. *Environmental Science & Technology*, 57(2), 1092–1102. https://doi.org/10.1021/acs.est.2c07303
12. Dopffel, N., Jansen, S., & Gerritse, J. (2021). Microbial side effects of underground hydrogen storage – Knowledge gaps, risks and opportunities for successful implementation. *International Journal of Hydrogen Energy*, 46(12), 8594–8606. https://doi.org/10.1016/j.ijhydene.2020.12.058
13. Dopffel, N., Mayers, K., Kedir, A., Alagic, E., An-Stepec, B. A., et al. (2023). Microbial hydrogen consumption leads to a significant pH increase under high-saline-conditions: Implications for hydrogen storage in salt caverns. *Scientific Reports*, 13(1), 10564. https://doi.org/10.1038/s41598-023-37630-y
14. Feio, M. J. (2004). *Desulfovibrio alaskensis sp. Nov.*, a sulphate-reducing bacterium from a soured oil reservoir. *International Journal of Systematic and Evolutionary Microbiology*, 54(5), 1747–1752. https://doi.org/10.1099/ijs.0.63118-0
15. Haddad, P. G., Ranchou-Peyruse, M., Guignard, M., Mura, J., Casteran, F., et al. (2022). Geological storage of hydrogen in deep aquifers – an experimental multidisciplinary study. *Energy & Environmental Science*, 15(8), 3400–3415. https://doi.org/10.1039/D2EE00765G
16. Halim, A., Shapiro, A., Lantz, A. E., & Nielsen, S. M. (2014). Experimental study of bacterial penetration into chalk rock: Mechanisms and effect on permeability. *Transport in Porous Media*, 101(1), 1–15. https://doi.org/10.1007/s11242-013-0227-x
17. Hill, D. D., & Sleep, B. E. (2002). Effects of biofilm growth on flow and transport through a glass parallel plate fracture. *Journal of Contaminant Hydrology*, 56(3–4), 227–246. https://doi.org/10.1016/S0169-7722(01)00210-8
18. Jangda, Z., Menke, H., Busch, A., Geiger, S., Bultreys, T., et al. (2023). Pore-scale visualization of hydrogen storage in a sandstone at subsurface pressure and temperature conditions: Trapping, dissolution and wettability. *Journal of Colloid and Interface Science*, 629, 316–325. https://doi.org/10.1016/j.jcis.2022.09.082
19. Kaster, K. M., Hiorth, A., Kjeilen-Eilertsen, G., Boccadoro, K., Lohne, A., et al. (2012). Mechanisms involved in microbially enhanced oil recovery. *Transport in Porous Media*, 91(1), 59–79. https://doi.org/10.1007/s11242-011-9833-7

20. Lankof, L., Luboń, K., Le Gallo, Y., & Tarkowski, R. (2024). The ranking of geological structures in deep aquifers of the Polish Lowlands for underground hydrogen storage. *International Journal of Hydrogen Energy*, 62, 1089–1102. https://doi.org/10.1016/j.ijhydene.2024.03.106
21. Liu, N., Kovscek, A. R., Fernø, M. A., & Dopffel, N. (2023). Pore-scale study of microbial hydrogen consumption and wettability alteration during underground hydrogen storage. *Frontiers in Energy Research*, 11, 1124621. https://doi.org/10.3389/fenrg.2023.1124621
22. Liu, N., Skauge, T., Landa-Marbán, D., Hovland, B., Thorbjørnsen, B., et al. (2019). Microfluidic study of effects of flow velocity and nutrient concentration on biofilm accumulation and adhesive strength in the flowing and no-flowing microchannels. *Journal of Industrial Microbiology and Biotechnology*, 46(6), 855–868. https://doi.org/10.1007/s10295-019-02161-x
23. Lysyy, M., Ersland, G., & Fernø, M. (2022). Pore-scale dynamics for underground porous media hydrogen storage. *Advances in Water Resources*, 163, 104167. https://doi.org/10.1016/j.advwatres.2022.104167
24. Nåmdal, M. B. (2023). *Microbial behavior and hydrogen consumption of Oleidesulfovibrio alaskensis—Implications for subsurface hydrogen storage* [Master thesis, The University of Bergen]. https://bora.uib.no/bora-xmlui/handle/11250/3074598
25. Oliver, M. C., Zheng, R., Huang, L., & Mehana, M. (2024). Molecular simulations of hydrogen diffusion in underground porous media: Implications for storage under varying pressure, confinement, and surface chemistry conditions. *International Journal of Hydrogen Energy*, 65, 540–547. https://doi.org/10.1016/j.ijhydene.2024.04.068
26. Oren, A. (2011). Thermodynamic limits to microbial life at high salt concentrations. *Environmental Microbiology*, 13(8), 1908–1923. https://doi.org/10.1111/j.1462-2920.2010.02365.x
27. Parsek, M. R., & Fuqua, C. (2004). Biofilms 2003: Emerging themes and challenges in studies of surface-associated microbial life. *Journal of Bacteriology*, 186(14), 4427–4440. https://doi.org/10.1128/JB.186.14.4427-4440.2004
28. Postgate, J. R. (1979). *The sulphate-reducing bacteria*. Cambridge Univ. Pr.
29. Rabbani, A., & Jamshidi, S. (2014). Specific surface and porosity relationship for sandstones for prediction of permeability. *International Journal of Rock Mechanics and Mining Sciences*, 71, 25–32. https://doi.org/10.1016/j.ijrmms.2014.06.013
30. Raza, A., Alafnan, S., Glatz, G., Arif, M., Mahmoud, M., & Rezk, M. G. (2022). Hydrogen diffusion in organic-rich porous media: Implications for hydrogen geo-storage. *Energy & Fuels*, 36(24), 15013–15022. https://doi.org/10.1021/acs.energyfuels.2c03070
31. Schiebahn, S., Grube, T., Robinius, M., Tietze, V., Kumar, B., & Stolten, D. (2015). Power to gas: Technological overview, systems analysis and economic assessment for a case study in Germany. *International Journal of Hydrogen Energy*, 40(12), 4285–4294. https://doi.org/10.1016/j.ijhydene.2015.01.123
32. Sharp, R. R., Cunningham, A. B., Komlos, J., & Billmayer, J. (1999). Observation of thick biofilm accumulation and structure in porous media and corresponding hydrodynamic and mass transfer effects. *Water Science and Technology*, 39(7), 195–201. https://doi.org/10.2166/wst.1999.0359
33. Sharp, R. R., Stoodley, P., Adgie, M., Gerlach, R., & Cunningham, A. (2005). Visualization and characterization of dynamic patterns of flow, growth and activity of biofilms growing in porous media. *Water Science and Technology*, 52(7), 85–90. https://doi.org/10.2166/wst.2005.0185
34. Stoodley, P., Sauer, K., Davies, D. G., & Costerton, J. W. (2002). Biofilms as complex differentiated communities. *Annual Review of Microbiology*, 56(1), 187–209. https://doi.org/10.1146/annurev.micro.56.012302.160705
35. Suthar, H., Hingurao, K., Desai, A., & Nerurkar, A. (2008). Evaluation of bioemulsifier mediated Microbial Enhanced Oil Recovery using sand pack column. *Journal of Microbiological Methods*, 75(2), 225–230. https://doi.org/10.1016/j.mimet.2008.06.007
36. Suthar, H., Hingurao, K., Desai, A., & Nerurkar, A. (2009). Selective plugging strategy-based microbial-enhanced oil recovery using Bacillus licheniformis TT33. *Journal of Microbiology and Biotechnology*, 19(10), 1230–1237.
37. Tarkowski, R. (2019). Underground hydrogen storage: Characteristics and prospects. *Renewable and Sustainable Energy Reviews*, 105, 86–94. https://doi.org/10.1016/j.rser.2019.01.051
38. Tarkowski, R., Lankof, L., Luboń, K., & Michalski, J. (2024). Hydrogen storage capacity of salt caverns and deep aquifers versus demand for hydrogen storage: A case study of Poland. *Applied Energy*, 355, 122268. https://doi.org/10.1016/j.apenergy.2023.122268
39. Taylor, S. W., & Jaffé, P. R. (1990). Biofilm growth and the related changes in the physical properties of a porous medium: 1. Experimental investigation. *Water Resources Research*, 26(9), 2153–2159. https://doi.org/10.1029/WR026i009p02153

40. Thaysen, E. M., McMahon, S., Strobel, G. J., Butler, I. B., Ngwenya, B. T., et al. (2021). Estimating microbial growth and hydrogen consumption in hydrogen storage in porous media. *Renewable and Sustainable Energy Reviews*, 151, 111481. https://doi.org/10.1016/j.rser.2021.111481
41. Thiyagarajan, S. R., Emadi, H., Hussain, A., Patange, P., & Watson, M. (2022). A comprehensive review of the mechanisms and efficiency of underground hydrogen storage. *Journal of Energy Storage*, 51, 104490. https://doi.org/10.1016/j.est.2022.104490
42. Tolker-Nielsen, T. (2015). Biofilm development. In: M. Ghannoum, M. Parsek, M. Whiteley, & P. K. Mukherjee (Eds.), *Microbial Biofilms* (pp. 51–66). ASM Press. https://doi.org/10.1128/9781555817466.ch3
43. UN.ESCAP, et. al. (2023) SDG 7: Affordable and clean energy. Retrieved from: https://hdl.handle.net/20.500.12870/5424.
44. Wikieł, A. J., Datsenko, I., Vera, M., & Sand, W. (2014). Impact of *Desulfovibrio alaskensis* biofilms on corrosion behaviour of carbon steel in marine environment. *Bioelectrochemistry*, 97, 52–60. https://doi.org/10.1016/j.bioelechem.2013.09.008
45. World Energy Outlook 2023 – Analysis. IEA. October 24, 2023. Accessed September 14, 2024. https://www.iea.org/reports/world-energy-outlook-2023
46. Yin, W., Wang, Y., Liu, L., & He, J. (2019). Biofilms: The microbial "protective clothing" in extreme environments. *International Journal of Molecular Sciences*, 20(14), 3423. https://doi.org/10.3390/ijms20143423
47. Yuan, W., Pan, Z., Li, X., Yang, Y., Zhao, C., et al. (2014). Experimental study and modelling of methane adsorption and diffusion in shale. *Fuel*, 117, 509–519. https://doi.org/10.1016/j.fuel.2013.09.046